Critical Behavior of the Metal-Insulator Transition in $La_{1-x}Sr_xMnO_3$

T. Okuda,[1] A. Asamitsu,[1] Y. Tomioka,[1] T. Kimura,[1] Y. Taguchi,[2] and Y. Tokura[1,2]
[1] *Joint Research Center for Atom Technology (JRCAT), Tsukuba 305-0046, Japan*
[2] *Department of Applied Physics, University of Tokyo, Tokyo 113-0033, Japan*

(Received 28 April 1998)

The critical behavior of the metal-insulator (MI) transition around $x_c = 0.16$ has been investigated for single crystals of $La_{1-x}Sr_xMnO_3$ by measurements of low-temperature resistivity and specific heat. The electronic specific heat coefficient, $\gamma = 3{-}5$ mJ/K^2 mol, indicates minimal mass-renormalization even near the MI transition whereas significant increases of the residual value and T^2 coefficient of resistivity as well as of T^3 term of specific heat are observed with a decrease of x toward x_c. The results indicate the presence of the spin-polarized anomalous metallic phase with strongly lattice- or orbital-coupled diffuse charge dynamics near x_c. [S0031-9007(98)07320-7]

PACS numbers: 71.30.+h, 72.15.Eb, 72.20.My, 75.70.Pa

Change of band filling or so-called carrier-doping procedure occasionally drives the metal-insulator (MI) transition in strongly correlated electron systems like perovskite-type transition metal oxides [1]. Among them, the carrier-doped manganese oxides with perovskite structure, $R_{1-x}A_xMnO_3$ (R and A being trivalent rare-earth and divalent ions, respectively), show versatile intriguing features arising from the mutual strong coupling among charge, spin, and lattice degrees of freedom [2]. A moderately hole-doped compound $La_{1-x}Sr_xMnO_3$ ($x \geq 0.18$) is believed to be the most canonical double-exchange ferromagnetic metal because of its relatively large bandwidth and the absence of such a long-range orbital ordering as observed in $LaMnO_3$ ($x = 0$). Late detailed experimental investigations have, however, been revealing novel features for the ferromagnetic ground state near the MI compositional boundary $x_c = 0.16$ [3,4]; for example, (1) a minimal Drude weight in the optical conductivity spectrum showing a dominant incoherent background [5], (2) a minimal quasiparticle weight at the Fermi level in the photoemission valence spectrum [6], (3) a fairly large T^2 coefficient of the resistivity [4], (4) a large variation of the residual resistivity with x and pressure [7,8]. Furthermore, in the MI critical region ($0.15 \leq x \leq 0.18$) the temperature dependence of resistivity shows anomalous upturn at a lower temperature than T_C (Curie temperature) as shown in Fig. 1, implying the occurrence of some order in the charge and/or orbital sector [8,9]. These features all remain to be elucidated in light of the importance of MI transition in this compound.

To argue the critical behavior of the MI transition in the ground state, we have investigated the low-temperature specific heat as well as the transport properties of $La_{1-x}Sr_xMnO_3$ crystals with finely controlled doping levels around the critical composition ($0.12 \leq x \leq 0.4$). Although the specific heat data were recently reported for polycrystalline samples of $La_{1-x}Sr_xMnO_3$ ($x = 0$, 0.1, 0.2, and 0.3) [10], we have tried to deduce accurate values of the electronic, magnetic, and lattice components by measurements under magnetic fields (up to 9 T) on high-quality single crystals with a fine interval of x near x_c to detect any possible anomaly upon the MI transition. In this paper, we report on the critical behavior around the MI phase boundary in comparison with the case of other filling-control MI transition systems, such as $V_{2-\delta}O_3$ [11] and $La_{1-x}Sr_xTiO_3$ [12].

Crystals of $La_{1-x}Sr_xMnO_3$ were grown by the floating-zone method. The details of growth conditions as well as structural and chemical characterizations of the obtained crystals have been published in previous papers [3,4]. Figure 1 shows the temperature (T) dependence of resistivity (ρ) of $La_{1-x}Sr_xMnO_3$ crystals in the region of x from 0.15 to 0.4. The resistivity with x above 0.18 is approximately proportional to T^2 at low temperatures ($T \leq 70$ K) and its T^2-coefficient A increases with the decrease of x to 0.18

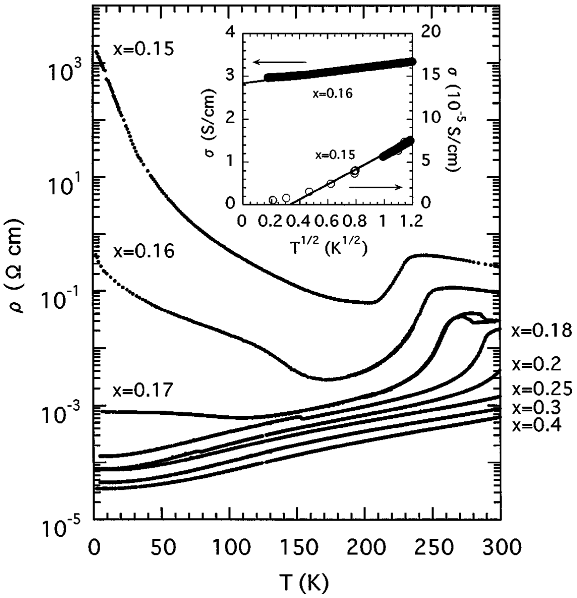

FIG. 1. Temperature dependence of resistivity of $La_{1-x}Sr_xMnO_3$ crystals. The inset shows the conductivity (inverse of resistivity) for the $x = 0.15$ and $x = 0.16$ crystals down to 35 mK plotted against $T^{1/2}$. Straight lines are a guide to the eyes.

(*vide infra*, and see also the top panel of Fig. 3). As the MI transition is approached with decrease of x, the upturn of the resistivity shows up for $0.15 \leq x \leq 0.18$ at lower temperatures than T_c as mentioned above. The T-dependent conductivity ($\sigma \equiv \rho^{-1}$) of the $x = 0.15$ and 0.16 crystals was measured down to 35 mK with use of a ^{3}He-^{4}He dilution refrigerator and is shown in the inset to Fig. 1. The σ values of both crystals are approximately proportional to $\sqrt{T}$ (solid lines), which suggests the Anderson localization effect, being typical of the interacting electron system [13]. The estimated conductivity at the absolute zero temperature (σ_0) is finite for $x = 0.16$ and zero for $x = 0.15$, signaling that the MI transition occurs at x in between 0.15 and 0.16.

Measurements of the specific heat (C) were done in the same crystals as used in the transport measurements by using the relaxation method from 0.5 to 20 K under various magnetic fields up to 9 T. In this paper we confine the arguments to the data above 3 K, in which contribution of the nucleus Schottky component [10] is negligible. Without the magnetic field and spin-wave gap, the specific heat in the ferromagnetic region in the temperature region from 3 to 10 K is then expressed as

$$C = \gamma T + \beta T^3 + B T^{3/2}. \qquad (1)$$

γ in the first term is the electronic specific heat coefficient, and the constant β in the second term relates to the Debye temperature Θ_D ($\propto \beta^{-1/3}$). The third term expresses the contribution of spin wave. In Fig. 2(a) we show the results for the $x = 0.15$ crystal in magnetic fields above 3 K. The specific heat shows a distinct decrease as the magnetic field increases. This reduction can be attributed to the suppression of the thermal excitation of the spin wave by a magnetic field. Then, under a magnetic field (H) the third term of Eq. (1) is modified as follows:

$$\begin{aligned} C_{\text{spin}} &= \frac{k_B^{5/2} T^{3/2}}{4\pi^2 D^{3/2}} F\left(\frac{H}{T}\right), \\ F\left(\frac{H}{T}\right) &= \int_{g\mu_B H}^{\infty} \frac{x^2 e^x}{(e^x - 1)^2} \sqrt{x - \frac{g\mu_B H}{k_B T}}\, dx. \end{aligned} \qquad (2)$$

In this equation the spin wave excitation at zero field is assumed to show no gap and follow the relation $\omega = Dq^2$, where D stands for the spin stiffness constant as determined from neutron scattering experiments [14]. In the inset to Fig. 2(a) is shown the reduction of C upon application of a field of 9 T, $\Delta C = C(0\text{ T}) - C(9\text{ T})$, for $x = 0.15$, which is compared with the calculated result (a solid line) based on Eq. (2). The field-induced reduction of specific heat can therefore be explained in terms of the suppressed contribution of the spin wave [15]. In this way we estimated the magnetic contribution to the specific heat.

The specific heat data, which were subtracted by the spin-wave component C_{spin} by the above procedure, are plotted as C/T versus T^2 for the $x = 0.15$, 0.2, and 0.3 crystals in Fig. 2(b) to see the electronic and lattice contributions. The data under several magnetic fields up to 9 T seem to fall on a single line within a small error for each x, indicating that the above estimate of the spin-wave component is fairly accurate. Thus estimated values of γ and Θ_D are plotted against x in Fig. 3 together with the inverse (σ_0) of the residual resistivity (ρ_0), the T^2-coefficient A of ρ ($= \rho_0 + AT^2$), and the Hall coefficient R_H at 4.2 K [16] in these compounds.

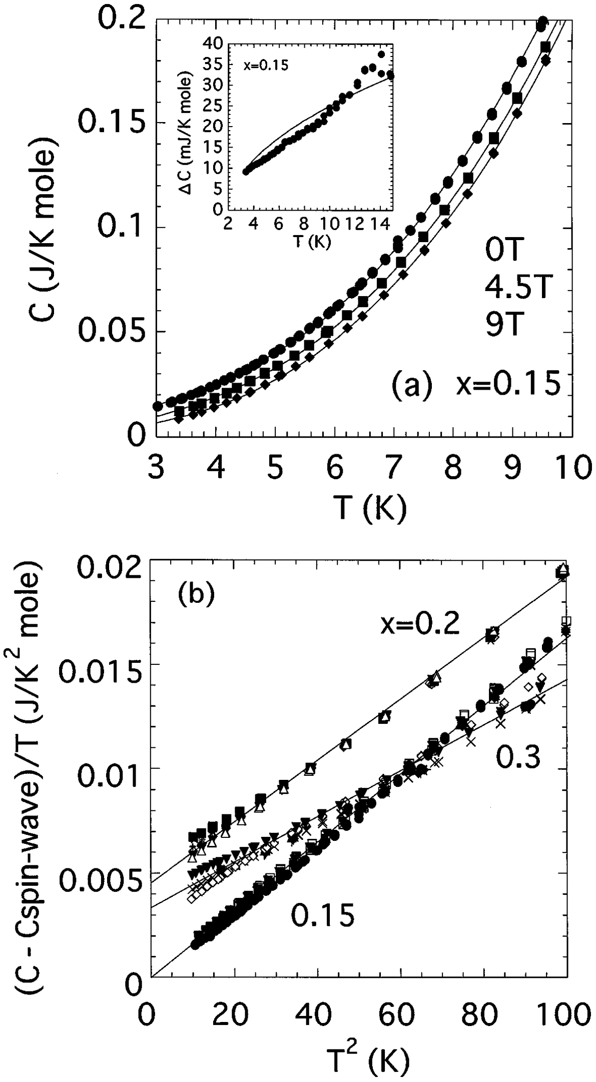

FIG. 2. (a) Specific heat (C) for $x = 0.15$ under magnetic fields. The inset shows reduction of C upon application of a field of 9 T for $x = 0.15$, and (b) C/T vs T^2 plot for $x = 0.15$, 0.2, and 0.3 where the spin-wave contribution is subtracted. Several symbols stand for the quantities under various magnetic fields (0–9 T).

The Debye temperature Θ_D is 360–440 K and significantly increases with the increase of x from 0.12 to 0.3, but appears to saturate above $x = 0.3$. The Θ_D values are comparable to those often found in perovskite oxides [17], but are smaller than the previous results, 430–490 K [10,18], while the tendency of the large increase of Θ_D with the increase of x from 0.1 to 0.3 is observed in the

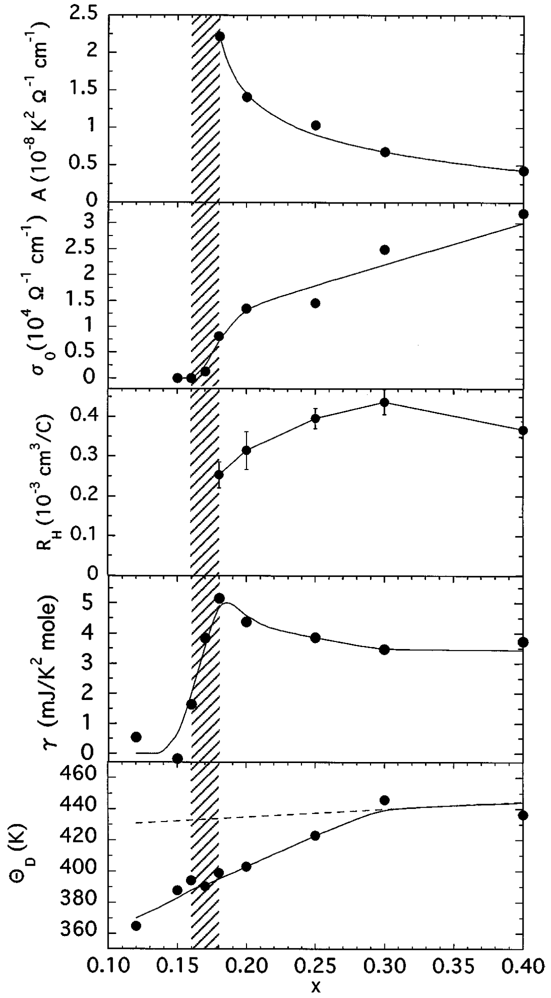

FIG. 3. Doping level (x) dependence of T^2 term coefficient A of resistivity, zero-temperature conductivity σ_0 (inverse of residual resistivity), Hall coefficient R_H, electronic specific heat coefficient γ, and Debye temperature Θ_D, for $\mathrm{La}_{1-x}\mathrm{Sr}_x\mathrm{MnO}_3$ crystals. A hatched vertical bar indicates the metal-insulator transitional region, where the resistivity upturn is observed at a lower temperature than T_C (Curie temperature).

both experiments [18]. Since the change in the density is small (less than 5%) with the variation of x from 0.1 to 0.3, the x dependence of Θ_D should be minimal as indicated by a dashed line in the bottom panel of Fig. 3. The change in Θ_D indicates that an anomalous softening of the lattice or increase of T^3-term in the specific heat occurs with the decrease of x in a fairly wide x region ($0.1 \leq x \leq 0.3$), but is not apparently relevant to the crystal structural (rhombohedral-orthorhombic) transition [19]. One of the possible accounts for this anomalous x-dependent change of Θ_D is to ascribe this lattice anomaly to the subsisting dynamic Jahn-Teller distortion down to low or zero temperature: In the region of $x = 0.1$–0.3 the collective Jahn-Teller distortion is quantum melted by hole motion as evidenced by the structural study [20], and accordingly the lattice stiffness may be much reduced as observed. The disappearance of the lattice anomaly above $x = 0.3$ implies that the orbital "moment" and the accompanying Jahn-Teller distortion becomes smaller in such an overdoped region with good metallicity.

The x variation of γ, whose relatively small error (± 0.5 mJ/K^2 mole) comes mainly from the estimate of the spin-wave contribution [15], is also shown in Fig. 3. The effective mass (m^*), derived from the γ and the band filling n ($= 1 - x$), is a few times larger than the bare mass (m_0) in the ferromagnetic metallic state, e.g., $m^*/m_0 \sim 2.5$ at $x = 0.3$, and does not critically increase around the MI critical point (x_c). This is in contrast with the conspicuous mass renormalization effect as observed for the other hole-doped transition metal oxides [1], e.g., $\mathrm{V_2O_3}$ [11], and $\mathrm{LaTiO_3}$ [12]. Figure 4 compares the x dependence of γ with that of $\mathrm{La}_{1-x}\mathrm{Sr}_x\mathrm{TiO}_3$ (or $\mathrm{LaTiO}_{3+x/2}$), in which the filling n of the conduction band (t_{2g}-state band) is $1 - x$ just as in the case of $\mathrm{La}_{1-x}\mathrm{Sr}_x\mathrm{MnO}_3$. A vertical hatching for this compound represents the antiferromagnetic (AF) metallic x region which is sandwiched by the AF insulating ($x \leq 0.05$) and paramagnetic metallic state ($x \geq 0.08$). Toward this magnetic instability point with a decrease of x, or as the Mott insulator ($x = 0$) is approached, the γ of $\mathrm{La}_{1-x}\mathrm{Sr}_x\mathrm{TiO}_3$ (or $\mathrm{LaTiO}_{3+x/2}$) is observed to critically increase, which indicates a canonical behavior of the Mott transition, namely the critical mass enhancement near the MI phase boundary [1,12]. For $x \geq 0.4$ being far from the MI boundary, γ of $\mathrm{La}_{1-x}\mathrm{Sr}_x\mathrm{MnO}_3$ is somewhat smaller than that of $\mathrm{La}_{1-x}\mathrm{Sr}_x\mathrm{TiO}_3$, which is simply thought to correspond to the difference of the bandwidth between Mn e_g and Ti t_{2g} bands in the nearly identical perovskite structure. Near the MI phase boundary, however, it is obvious that the increase of γ is much less in $\mathrm{La}_{1-x}\mathrm{Sr}_x\mathrm{MnO}_3$ than in $\mathrm{La}_{1-x}\mathrm{Sr}_x\mathrm{TiO}_3$. Thus, the MI transition in $\mathrm{La}_{1-x}\mathrm{Sr}_x\mathrm{MnO}_3$ is not a prototypical filling-control MI transition in correlated electron systems.

We might argue that the half-metallic nature with full spin polarization in this compound is responsible for such

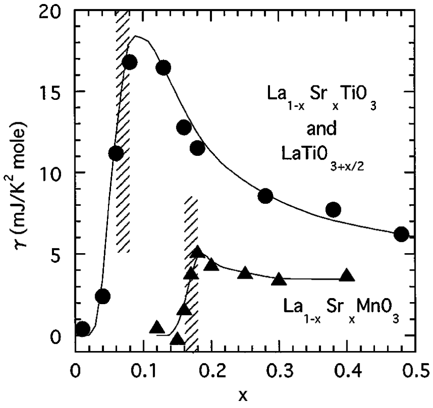

FIG. 4. Doping level (x) dependence of γ for $\mathrm{La}_{1-x}\mathrm{Sr}_x\mathrm{MnO}_3$ compared with that for $\mathrm{La}_{1-x}\mathrm{Sr}_x\mathrm{TiO}_3$ ($\mathrm{LaTiO}_{3+x/2}$). For a hatched vertical bar for $\mathrm{La}_{1-x}\mathrm{Sr}_x\mathrm{TiO}_3$ (or $\mathrm{LaTiO}_{3+x/2}$), see the text. For the hatched x region for $\mathrm{La}_{1-x}\mathrm{Sr}_x\mathrm{MnO}_3$, see the caption of Fig. 3.

a behavior, since the mass enhancement mechanism arising from the spin fluctuation as in the nearly antiferromagnetic metal [21] is missing in this compound. Furthermore, as far as the metallic region ($x \geq 0.18$) without resistivity upturn is concerned, R_H (midpanel of Fig. 3) remains at a small positive value (corresponding to nominally ~1 hole/Mn), being typical of a metal with a large Fermi surface. Nevertheless, as shown in Fig. 3, the T^2 coefficient A of the ρ rather steeply increases with decrease of x, which is naively interpreted as a signal of the importance of the electron correlation. (The magnon scattering usually gives rise to the T dependence of resistivity with a higher power, say $\rho \propto T^{9/2}$ [22].) However, the ratio of A to γ^2 is about $7 \times 10^{-10}\ \Omega\,\mathrm{cm}\,(\mathrm{mol\,K/mJ})^2$, which is about 70 times as large as the universal constant in Kadowaki-Wood's law [23] for the strongly correlated electron systems. A plausible candidate of such a strong scatterer of the carriers in the almost fully spin-polarized state is the orbital fluctuation in the doubly degenerate e_g state [24,25] or the relevant coupling to the lattice distortion (Jahn-Teller type). However, it is left to be theoretically elucidated that such a specific mechanism can lead to the observed T^2 dependence of the resistivity.

Scrutinizing the immediate vicinity ($x = 0.15$–0.18) of the MI phase boundary (a hatched region in Figs. 3 and 4) where the resistivity upturn is observed (see Fig. 1), we note that the γ value rather decreases continuously with the decrease of x from 0.18 to 0.15, and becomes zero around at $x = 0.15$. Thus the Fermi surface gradually shrinks towards the insulating phase and finally disappears at the MI phase boundary. The observed decrease of σ_0 (inverse of the residual resistivity) with x from $x = 0.18$ to $x = 0.15$ (in the hatched region of Fig. 3) is in accord with this tendency, but is too steep to be all ascribed to the density of state effect. This suggests that the MI transition in the immediate vicinity around $x_c = 0.16$ is also affected by the Anderson localization effect [13], as is also evidenced by the $T^{1/2}$ dependence of the conductivity (argued in the inset to Fig. 1).

In conclusion, the MI transition in $\mathrm{La}_{1-x}\mathrm{Sr}_x\mathrm{MnO}_3$ around $x_c = 0.16$ appears to be driven by the gradual disappearance of the Fermi surface without significant increase of γ. The residual resistivity, the T^2 term coefficient A of resistivity, and T^3 term of specific heat are anomalously enhanced while keeping the ratio of A/γ^2 anomalously large, as the ferromagnetic insulating phase is approached from higher x. Such a highly diffuse dynamics of the fully spin-polarized carriers in these manganites is likely to arise from the dynamically but collectively orbital-ordered or Jahn-Teller-distorted background which is manifested by anomalous softening of the lattice, i.e., enhanced T^3 term in specific heat.

We are grateful to N. Nagaosa and M. Imada for enlightening discussions and to N. Wada for his helpful advice on the specific heat measurement. This work was supported by the New Energy and Industrial Technology Development Organization of Japan (NEDO) and also by a Grant-In-Aid for Scientific Research from the Ministry of Education, Science, Sports, and Culture, Japan.

[1] For a review, see, for example, M. Imada, A. Fujimori, and Y. Tokura, Rev. Mod. Phys. (to be published).

[2] For a review, see, for example, *Colossal Magnetoresistive Oxides,* edited by Y. Tokura (Gordon and Breach Science, New York, to be published).

[3] Y. Tokura *et al.,* J. Phys. Soc. Jpn. **63**, 3931 (1994).

[4] A. Urushibara *et al.,* Phys. Rev. B **51**, 14 103 (1995).

[5] Y. Okimoto *et al.,* Phys. Rev. B **55**, 4206 (1997).

[6] D. D. Sarma *et al.,* Phys. Rev. B **53**, 6873 (1996).

[7] Y. Moritomo *et al.,* Phys. Rev. B **56**, 12 190 (1997).

[8] J.-S. Zhou *et al.,* Phys. Rev. Lett. **79**, 3234 (1997).

[9] Y. Yamada *et al.,* Phys. Rev. Lett. **77**, 904 (1996).

[10] B. F. Woodfield *et al.,* Phys. Rev. Lett. **78**, 3201 (1997).

[11] D. B. McWhan *et al.,* Phys. Rev. B **2**, 3734 (1970); **7**, 1920 (1973).

[12] Y. Tokura *et al.,* Phys. Rev. Lett. **70**, 2126 (1993); K. Kumagai *et al.,* Phys. Rev. B **48**, 7636 (1993); Y. Taguchi *et al.,* (unpublished).

[13] P. A. Lee and T. V. Ramakrishnan, Rev. Mod. Phys. **57**, 287 (1985).

[14] K. Hirota *et al.,* Physica (Amsterdam) **237B–238B**, 36 (1997); Y. Endoh and K. Hirota, J. Phys. Soc. Jpn. **66**, 2264 (1997).

[15] In the case of the metallic ferromagnet such as the $x = 0.18$ crystal, we have analyzed all the results by assuming the constant gap at $q = 0$ in spin-wave excitation, such that $\omega = Dq^2 + \Delta_{\mathrm{spin}}$. The estimated value of the Δ_{spin} term, for example 1.7 meV Å^2 for the $x = 0.3$ crystal, is roughly consistent with that used for the fitting of the spin-wave dispersion in the neutron scattering measurements [14].

[16] A. Asamitsu and Y. Tokura, Phys. Rev. B **58**, 47 (1998).

[17] K. P. Rajeev and A. K. Raychaudhauri, Solid State Commun. **79**, 591 (1991); J. J. Hamilton *et al.,* Phys. Rev. B **54**, 14 926 (1966).

[18] In the original report [10], Θ_D is 255–285 K, based on a different definition of Θ_D and here is shown as multiplied by $5^{1/3}$.

[19] A. Asamitsu *et al.,* Nature (London) **373**, 407 (1995); A. Asamitsu *et al.,* Phys. Rev. B **54**, 1716 (1996).

[20] H. Kawano *et al.,* Phys. Rev. B **53**, R14 709 (1996); Phys. Rev. B **53**, 2202 (1996).

[21] K. Ueda, J. Phys. Soc. Jpn. **43**, 1497 (1977); T. Moriya, in *Proceedings of the 17th Taniguchi Symposium: Spectroscopy of Mott Insulators and Correlated Materials, Kashikojima, Japan, 1994,* edited by A. Fujimori and Y. Tokura, Springer Series in Solid-State Sciences (Springer, Berlin, 1995), p. 66.

[22] K. Kubo and N. Ohata, J. Phys. Soc. Jpn. **33**, 21 (1972).

[23] K. Kadowaki and S. B. Woods, Solid State Commun. **58**, 507 (1986).

[24] M. Imada, J. Phys. Soc. Jpn. **67**, 45 (1998); S. Ishihara *et al.,* Phys. Rev. B **56**, 686 (1997).

[25] S. Ishihara *et al.,* Phys. Rev. B **56**, 686 (1997).